

Different Roles of Electrostatics in Heat and in Cold: Adaptation by Citrate Synthase

Sandeep Kumar^[a, b] and Ruth Nussinov^{*[a, c]}

*Electrostatics plays a major role in heat adaptation by thermophilic proteins. Here we ask whether electrostatics similarly contributes to cold adaptation in psychrophilic proteins. We compare the sequences and structures of citrate synthases from the psychrophile *Arthobacter Ds2-3R*, from chicken, and from the hyperthermophile *Pyrococcus furiosus*. The three enzymes share similar packing, burial of nonpolar surface area, and main-chain hydrogen bonding. However, both psychrophilic and hyperthermophilic citrate synthases contain more charged residues, salt bridges, and salt-bridge networks than the mesophile. The electrostatic free-energy contributions toward protein stability by individual charged residues show greater variabilities in the psychrophilic citrate synthase than in the hyperthermophilic enzyme. The charged residues in the active-site regions of the psychrophile are more destabilizing than those in the active-site regions of the hyper-*

thermophile. In the hyperthermophilic enzyme, salt bridges and their networks largely cluster in the active-site regions and at the dimer interface. In contrast, in the psychrophile, they are more dispersed throughout the structure. On average, salt bridges and their networks provide greater electrostatic stabilization to the thermophilic citrate synthase at 100 °C than to the psychrophilic enzyme at 0 °C. Electrostatics appears to play an important role in both heat and cold adaptation of citrate synthase. However, remarkably, the role may be different in the two types of enzyme: In the hyperthermophile, it may contribute to the integrity of both the protein dimer and the active site by possibly countering conformational disorder at high temperatures. On the other hand, in the psychrophile at low temperatures, electrostatics may contribute to enhance protein solvation and to ensure active-site flexibility.

Introduction

Living organisms can be roughly classified into psychrophiles (living temperature, $T_L \approx 0-15^\circ\text{C}$), mesophiles ($T_L \approx 20-40^\circ\text{C}$), and thermophiles ($T_L \approx 60^\circ\text{C}$ or higher). Among the thermophiles, organisms with living temperatures near the boiling point of water or higher are referred to as hyperthermophiles. At the molecular level, the increasing availability of sequence, structural, thermodynamic, and biochemical information about proteins from thermophilic and psychrophilic organisms facilitates understanding of how the temperature adaptation is achieved. How thermophilic proteins deal with heat^[1] is better understood than how psychrophilic proteins tolerate cold. This is due to the greater availability of data on thermophiles and thermophilic proteins. Complete genome sequences are now available for several thermophilic organisms^[1a] and factors for enhanced thermostability have been intensively investigated.^[2] The higher melting temperatures of the thermophilic proteins are often accompanied by greater thermodynamic stabilities than those of the mesophilic homologues.^[2a] Among the various factors suggested for the greater stability of the thermophilic proteins, the most consistent is the better optimized protein electrostatics.^[1-3] Protein electrostatics refers to the distribution of the charged and polar residues in the protein structure and their interactions. The improvement in protein electrostatics may come from 1) a single charged residue that relieves electrostatic repulsion,^[1c, 3c, 4] 2) increased formation of salt bridges and their networks,^[1a,b, 2] and 3) greater electrostatic contribution to the


stability of the thermophilic proteins by salt bridges and their networks.^[2c, 3a, 3f]

Only limited data are available for psychrophilic proteins^[5] and there is no completed genome sequence. The adaptation to low temperatures is thought to be achieved through reduction in the activation energy and increased catalytic efficiency,^[6a] probably due to greater flexibility, either overall or in selected region(s).^[6] Model building studies of psychrophilic proteins from homologous mesophilic/thermophilic protein template(s) indicate the occurrence of fewer hydrogen bonds, salt bridges/ion pairs, and salt-bridge networks, as seen, for example, in 3-isopropyl malate

[a] Dr. S. Kumar, Prof. R. Nussinov
Basic Research Program, SAIC-Frederick, Inc.
Laboratory of Experimental and Computational Biology
NCI-Frederick, Building 469, Room 151, Frederick, MD 21702 (USA)
Fax: (+1) 301-846-5598
E-mail: ruthn@ncifcrf.gov

[c] Dr. S. Kumar
Current address:
LR3, PCS Building, Georgetown University Medical Center
3900 Reservoir Road, Washington DC 20057 (USA)

[b] Prof. R. Nussinov
Sackler Institute of Molecular Medicine
Department of Human Genetics and Molecular Medicine
Sackler Faculty of Medicine, Tel Aviv University
Tel Aviv 69978 (Israel)

 Supporting information for this article is available on the WWW under <http://www.chembiochem.org> or from the author.

dehydrogenase.^[7] Chen and Berns^[8] have reported that the psychrophilic phycocyanin is more susceptible to urea denaturation than the homologous thermophilic, mesophilic, and halophilic phycocyanins are. Recently, microcalorimetric experiments by Lonhienne et al.^[9] have indicated that only the active-site domain of psychrophilic Chitobiase is heat labile. At present, it is difficult to say if the psychrophilic proteins have lower thermodynamic stability than their mesophilic and/or thermophilic homologues. Furthermore, there are no estimates of the differential thermodynamic stabilities among protein families containing homologous psychrophilic, mesophilic, and thermophilic proteins. However, progress is being made in solving the crystal structures of psychrophiles and comparative studies with mesophilic and thermophilic proteins are increasingly available.^[5, 10]

While the role of electrostatics in enhancing protein thermostability has been well studied, their possible contribution towards active-site flexibility and proper solvation of the psychrophilic proteins at low temperatures has not been appreciated. Here we study citrate synthase (E.C. 4.1.3.7) which catalyzes the condensation of acetyl-coenzyme A and oxaloacetate into citrate and coenzyme A in the citric acid cycle.^[10e, 11] We use homologous enzymes from the psychrophilic antarctic bacterium *Arthobacter* Ds2–3R,^[10a] from chicken heart muscle,^[12] and from the hyperthermophile *Pyrococcus furiosus*. We focus mainly on the similarities and differences between psychrophilic and hyperthermophilic citrate synthases. The psychrophilic and hyperthermophilic enzymes share larger sequence and structural similarities with each other than with the mesophilic citrate synthase. Both the psychrophilic and hyperthermophilic citrate synthases contain higher proportions of charged residues and salt bridges than the mesophilic citrate synthase, even though the size of the mesophile is bigger. These observations indicate that electrostatics plays important roles in both heat and cold adaptation by citrate synthase. In the hyperthermophile, the higher occurrence of salt bridges and their networks may resist conformational disorder around the active site and at the dimer interface. In the psychrophile, the overall increased occurrence of charged residues throughout the structure should ensure proper solvation at low temperatures. Here, the salt bridges and their networks are more dispersed throughout the 3D structure and the charged active-site residues are electrostatically more destabilizing, which possibly leads to a greater conformational flexibility.

Results

Citrate synthase is among the well-studied enzymes in biochemistry. In the summer of 2002, the Protein Data Bank (PDB;^[13] <http://www.rcsb.org/pdb/>) contained 20 crystal structures of citrate synthase and 44 complete amino acid sequences were available from SWISS-PROT (<http://www.expasy.ch/sprot/sprot-top.html>). We have selected three homologous citrate synthases from the hyperthermophile *Pyrococcus furiosus* (PfCs),^[14] the mesophile *Gallus gallus* (chicken; GgCs, ref. [12]), and the psychrophilic antarctic bacterium *Arthobacter* Ds2–3R (DsCs, ref. [10a]) for our study. The optimum growth temperature of

Arthobacter Ds2–3R is 0 °C, that of *Pyrococcus furiosus* is approximately 100 °C, and the body temperature of chicken is 41 °C. The psychrophilic citrate synthase is optimally active at 31 °C and inactivates at 45 °C.^[10a] In contrast, the hyperthermophilic one has a half life of 17 minutes at 100 °C.^[14] At 6 °C, DsCs is 29 times more active than PfCs.^[10a] The availability of these data enables the use of citrate synthase as a model system for studies of heat and cold adaptation. Previously, Russell et al.^[10a] have rationalized the differences in PfCs and DsCs on the basis of 1) a larger dimeric interface in PfCs, 2) formation of complex ion pairs and isoleucine and tyrosine clusters at the PfCs dimer interface, 3) removal of prolines from the DsCs loop regions, and 4) longer surface loops containing charged residues in DsCs.

Sequence and structural comparisons of psychrophilic, mesophilic, and hyperthermophilic citrate synthases

DsCs has a higher sequence and structural similarity with PfCs than with GgCs (Figure 1). DsCs has 41% sequence identity and 1.26 Å C α atom root mean square deviation (RMSD) with PfCs, as compared to 28.7% and 1.68 Å with GgCs. The amino acid sequence of DsCs also shows approximately 34% sequence

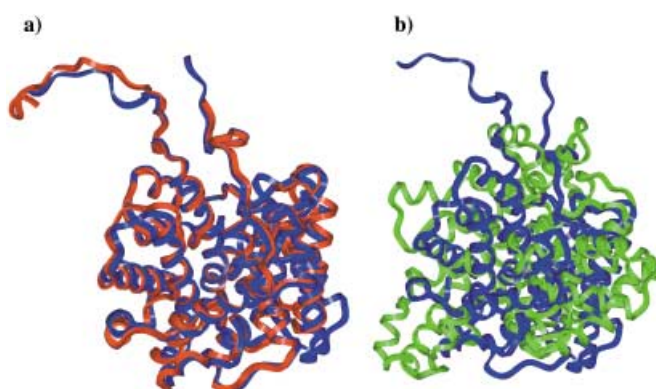


Figure 1. Ribbon diagrams showing the superposition of the psychrophilic citrate synthase (DsCS; blue) on a) hyperthermophilic citrate synthase (PfCs; red) and b) chicken citrate synthase (GgCs; green). Only the monomeric protein chains are shown. DsCS and PfCs are more similar to each other than they are to GgCs.

identities with citrate synthases from *Sulfolobus solfataricus* and *Thermoplasma acidophilum* (data not shown). The sequence and structural similarities between DsCs and PfCs enable us to compare their differences for cold and heat adaptation with greater confidence. Table 1 presents a comparison of the three citrate synthases. Atomic packing and burial of nonpolar surfaces are similar in the three enzymes. The individual polypeptide chains of DsCs and PfCs are approximately 60 residues shorter than those of GgCs. When the differences in protein size are taken into account, all three show similar extents of main-chain/main-chain and main-chain/side-chain hydrogen bonding and polar, nonpolar, and total surface areas for the monomeric and dimeric forms. DsCs has a smaller subunit interface than PfCs, even though both proteins are approximately the same size (Table 1 and ref. [10a]). However, the polar

Table 1. Comparison of sequence composition and structural properties among psychrophilic, mesophilic, and hyperthermophilic citrate synthases.

Property	DsCs	GgCs	PfCs
PDB entry	1A59	1CSH	1AJ8
resolution [Å]	2.09	1.60	1.9
molecule in crystal asymmetric unit	monomer	monomer	dimer
biologically active state	dimer	dimer	dimer
N_{res} (monomer) ^[a]	378	437	376
hydrophobicity [%] ^[b]	87	88	82
compactness ^[c]	1.99	1.93	2.04
%(D + E + K + R) ^[d]	23.3	18.8	26.1
%(A + I + L + V) ^[d]	31.7	30.7	32.4
%(F + W + Y) ^[d]	8.0	11.0	11.1
%P ^[d]	4.8	5.5	4.6
%G ^[d]	5.8	8.3	7.8
MC – MC HB ^[e]	494	566	490
MC – SC HB ^[e]	194	228	197
SC – SC HB ^[e]	56	48	39
salt bridges (SB) ^[f]	26	12	20
intrachain SB ^[f]	24	10	15
interchain SB ^[f]	2	2	5
salt-bridge networks ^[f]	2	0	2
intrachain networks ^[f]	2	0	1
interchain networks ^[f]	0	0	1
B factors [Å ²] ^[g]	13.6 ± 8.4	13.8 ± 9.0	20.0 ± 6.0 (chain A) 22.2 ± 9.6 (chain B)
ASA _{monomer} ^{tot} [Å ²] ^[h]	18391.4	20624.3	18732.4 (chain A) 18822.8 (chain B)
ASA _{monomer} ^{pol} [Å ²] ^[h]	8616.0	9718.1	8782.4 (chain A) 8836.5 (chain B)
ASA _{monomer} ^{nonpol} [Å ²] ^[h]	9775.4	10906.2	9950.0 (chain A) 9986.3 (chain B)
ASA _{dimer} ^{tot} [Å ²] ^[h]	28556.4	31702.2	28510.2
ASA _{dimer} ^{pol} [Å ²] ^[h]	13854.6	15607.7	14024.7
ASA _{dimer} ^{nonpol} [Å ²] ^[h]	14701.8	16094.5	14485.5
ASA _{intfc} ^{tot} [Å ²] ^[h]	8226.4	9546.5	9045.0
ASA _{intfc} ^{pol} [Å ²] ^[h]	3377.5	3828.5	3594.2
ASA _{intfc} ^{nonpol} [Å ²] ^[h]	4848.9	5718.0	5450.8

[a] The number of residues in one subunit of citrate synthase. [b] The extent of nonpolar surface area buried in the protein. The values shown here are for citrate synthase dimers. [c] A measure of atomic packing in the citrate synthase dimers. A smaller value indicates better packing. [d] Percentages of charged (Asp, Glu, Lys, and Arg), apolar (Ala, Ile, Leu, and Val), aromatic (Phe, Trp, and Tyr), proline, and glycine residues in citrate synthase sequences. The amino acids are indicated with the single letter code. [e] The numbers of main-chain/main-chain (MC – MC), main-chain/side-chain (MC – SC), and side-chain/side-chain (SC – SC) hydrogen bonds (HB) in citrate synthase dimers. [f] The numbers of intra- (within subunits) and interchain (across subunits) salt bridges and their networks in the citrate synthase dimers. [g] Average values of B factors for $C\alpha$ atoms for the protein chains in the crystallographic asymmetric units of citrate synthases. [h] ASA stands for accessible surface area. The polar (pol), nonpolar (nonpol) and total (tot) ASA values were computed for both monomers (monomer) and dimers (dimer). This allows estimation of polar and nonpolar protein surface area buried in the subunit interfaces (intfc) of the citrate synthases.

and nonpolar surfaces are buried with similar proportions ($\approx 40:60$) in the subunit interfaces of DsCs and PfCs. These proportions are also similar for GgCs. The average values of crystallographic B factors for $C\alpha$ atoms in DsCs, GgCs, and PfCs are similar. PfCs and DsCs have similar B -factor values for main-chain and side-chain atoms.^[10a] Despite the 41% sequence

identity between DsCs and PfCs, the amino acid distributions in the two proteins are significantly different. A χ^2 test^[15] between the DsCs and PfCs sequences yields a value of 68.79. To allow the null hypothesis (H_0) that the two distributions are similar to be rejected at a 95% level of confidence (probability of accepting the null hypothesis, $p \leq 0.05$), the χ^2 value for 19-parameter systems such as protein sequences should be greater than 30.14.

Both DsCs and PfCs contain a greater proportion of charged residues (Asp, Glu, Lys, and Arg) than the mesophile GgCs (Table 1). An increase in the proportion of charged residues is well known for thermophilic proteins,^[1a, b, 2b] but not for psychrophilic ones. The proportion of charged residues in DsCS (23.3%) is smaller than that in PfCs (26.1%). The three enzymes contain similar proportions of aliphatic residues (Ala, Ile, Leu, and Val). DsCs contains a smaller proportion of aromatic residues (Phe, Trp, and Tyr) than GgCs and PfCs. The proportion of prolines is similar in DsCS and PfCs. Although DsCs is expected to be more flexible than GgCs and PfCs, the proportion of Gly residues is smaller in DsCs than either GgCs or PfCs (Table 1). However, the locations of Gly and Pro residues in PfCs and DsCs are different.^[10a] Between PfCs and DsCs, a change-of-proportion test^[15] shows the increase in the proportion of Ala ($\Delta = 4.9\%$ for DsCs) and the decrease in the proportions of Ile (-5.2%), Lys (-3.9%), and Tyr (-3.3%) to be statistically significant at the 95% level of confidence.

The psychrophilic citrate synthase dimer contains 26 salt bridges while the hyperthermophile contains 20. Most (24 out of 26) of the salt bridges in DsCs are formed within the subunits and only two are formed across the interface. On the other hand, 5 out of the 20 salt bridges in PfCs are across the dimer interface (Table 1). DsCs contains one salt-bridge triad within each subunit. PfCs also contains two salt-bridge triads, one of which is across the dimer interface. Hence, even though both PfCs and DsCs show increased formation of salt bridges and their networks, the location of these interactions are different in the two proteins. Figure 2 shows the locations of residues forming salt bridges (shown in ball and stick representation) in PfCs and DsCs. In PfCs, the majority of the salt bridges and their networks are formed around the active site (shown as a CPK representation) and the dimer interface (Figure 2a). In contrast, the salt bridges and their networks are more dispersed throughout the DsCs structure (Figure 2b). The chicken citrate synthase contains 12 salt bridges, with 2 at the dimer interface.

Electrostatic profiles of hyperthermophilic, mesophilic, and psychrophilic citrate synthases

Calculations of the electrostatic free-energy contribution towards protein stability ($\Delta\Delta G_{\text{elec-chrs}}$) by individual charged residue can help identify potential stabilizing and destabilizing charged residues in a protein. $\Delta\Delta G_{\text{elec-chrs}}$ is the sum of two terms, $\Delta\Delta G_{\text{dslv-chrs}}$ and $\Delta\Delta G_{\text{prt-chrs}} \cdot \Delta\Delta G_{\text{dslv-chrs}}$ measures the energy penalty due to the desolvation of a charged residue in the folded state of the protein as compared to its unfolded state and $\Delta\Delta G_{\text{prt-chrs}}$ is the free-energy change due to the interaction of the side-chain functional group in the charged residue with the other charges in the rest of the protein. For each charged residue, the $\Delta\Delta G_{\text{elec-chrs}}$

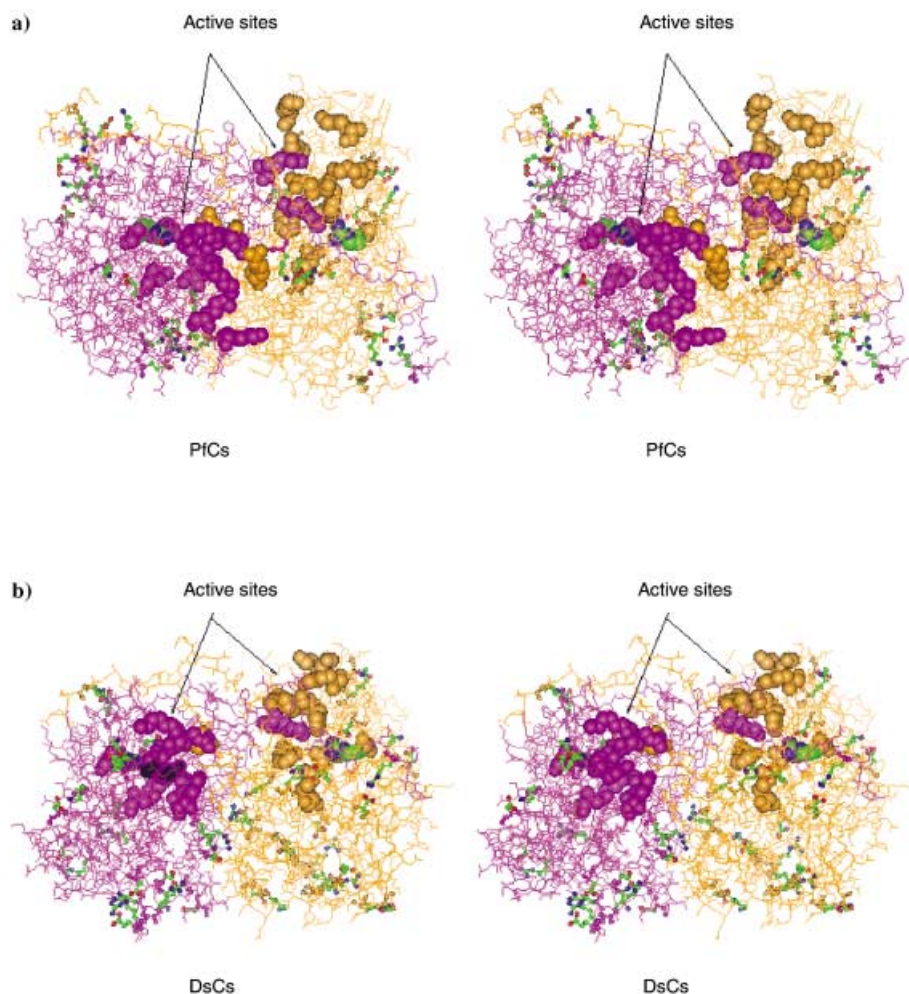


Figure 2. Diagrams showing the location of residues forming salt bridges and their networks in a) hyperthermophilic (PfCs) and b) psychrophilic (DsCs) citrate synthases. The individual polypeptide chains of the dimers are shown in golden and magenta. The charged residues involved in salt bridges are shown as ball and stick representations, except those which also form part of the binding sites. All the residues involved in citrate and coenzyme A binding sites are shown as CPK representations. For all the salt-bridge-forming charged residues, the backbone atoms are shown in the colors of their respective polypeptide chains but the identities of the side-chain atoms are color coded. The oxygen atoms are in red, the nitrogen atoms are in blue, and the carbon atoms are in green. The rest of the protein structure is shown by thin sticks. The salt bridges and their networks tend to concentrate around the active-site region and in the dimer interface of PfCs. These interactions are dispersed throughout the structure in DsCs.

value was computed with respect to the residue's hydrophobic isostere, which is the charged residue with its side-chain partial atomic charges set to zero. The Experimental Section presents the detailed procedure followed in these calculations.

We have calculated the $\Delta\Delta G_{\text{elec-chrs}}$ values for each of the charged residues (Asp, Glu, Lys, and Arg) in DsCs (176 residues), GgCs (164 residues), and PfCs (195 residues) dimers. Histidines were not included in this analysis. The protein and water dielectric constants were taken to be 4 and 80, respectively. The $\Delta\Delta G_{\text{elec-chrs}}$ values for all three proteins correspond to the values at 25 °C to facilitate direct comparisons among DsCs, GgCs, and PfCs. The average $\Delta\Delta G_{\text{elec-chrs}}$ values of subunits A and B are -1.7 ± 8.8 and -1.5 ± 8.9 kcal mol⁻¹, respectively, in DsCs; -2.3 ± 9.3 and -2.2 ± 8.6 kcal mol⁻¹, respectively, in GgCs; and -1.0 ± 6.6 and -1.3 ± 6.0 kcal mol⁻¹, respectively, in PfCs. The

above values summarize the results of several hundred electrostatics calculation sets and the large standard deviations about the mean values do not indicate error bars for our calculations. Rather, they indicate a wide scatter in the electrostatic free-energy contributions by the individual charged residues in these proteins. This scatter arises due to the diversity in side-chain functional-group orientation as well as the location of the different charged residues in the protein. The differences in structural context of the individual charged residues also contribute towards this scatter. The electrostatic profile, a plot of $\Delta\Delta G_{\text{elec-chrs}}$ with respect to the residue number, allows a comparison of electrostatic free-energy contributions by individual charged residues. Figure 3 compares the electrostatic profiles of the psychrophilic (DsCs) and hyperthermophilic (PfCs) citrate synthases. The figure shows electrostatic profiles for each protein chain in PfCs and DsCs. The profiles show large variabilities in the $\Delta\Delta G_{\text{elec-chrs}}$ values for the individual charged residues. However, there are greater variations in the electrostatic profiles of DsCs than those of PfCs. The electrostatic profiles of GgCs (mesophile) also have large variabilities (not shown), but the variations are smaller than those observed in DsCs. Figure 4 presents a comparison of electrostatic profiles for PfCs and DsCs dimer structures in a color-coded form. At the respective living temperatures of the enzymes, the $\Delta\Delta G_{\text{elec-chrs}}$ values for the charged residues should change, since the dielectric constant of water (ϵ_w) increases

to 87.90 at 0 °C and decreases to 55.51 at 100 °C.^[16] This would further reduce the variabilities in the electrostatic profile of PfCs but increase in that of DsCs.

In all three citrate synthases, the number of stabilizing ($\Delta\Delta G_{\text{elec-chrs}} < 0$) charged residues (PfCs, 111; DsCs, 105; GgCs, 93) is greater than the number of destabilizing ($\Delta\Delta G_{\text{elec-chrs}} > 0$) charged residues (PfCs, 84; DsCs, 71; GgCs, 71) and the ratios of stabilizing to destabilizing charged residues are similar (PfCs, 1.3; DsCs, 1.4; GgCs, 1.3).

We arbitrarily take a charged residue to be significantly stabilizing/destabilizing if $|\Delta\Delta G_{\text{elec-chrs}}| \geq 5$ kcal mol⁻¹. Each plot in Figure 3 shows horizontal lines drawn at $\Delta\Delta G_{\text{elec-chrs}} = \pm 5$ kcal mol⁻¹ to indicate significantly stabilizing/destabilizing residues. There are notable differences in the occurrence of residues with large magnitudes of electrostatic free-energy

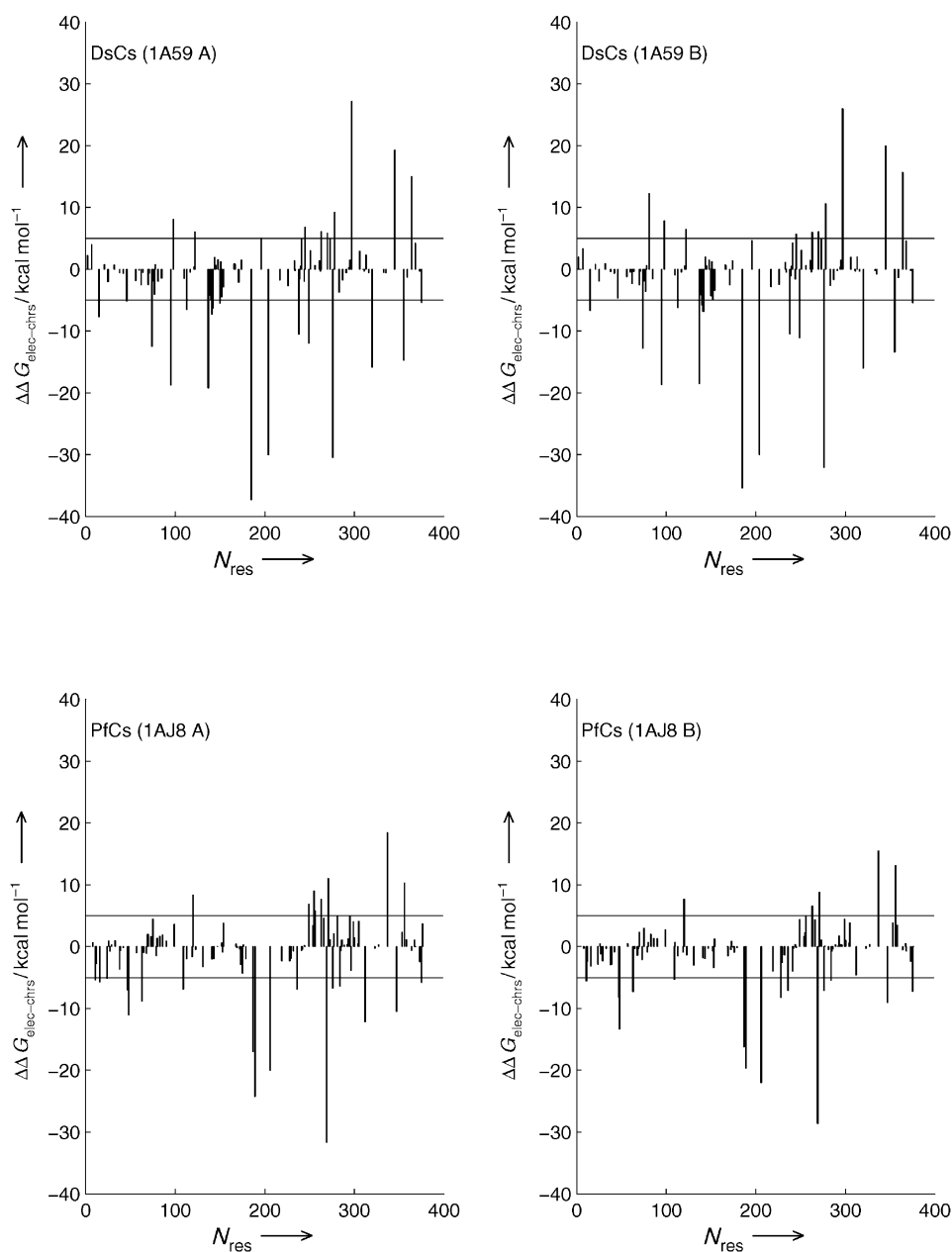


Figure 3. Plots showing the electrostatic free-energy contribution of the charged residues (Asp, Glu, Lys, Arg) toward protein stability. In each plot, the X axis denotes the residue number and the Y axis denotes the electrostatic free-energy contribution ($\Delta\Delta G_{\text{elec-chrs}}$). The horizontal lines indicate $\Delta\Delta G_{\text{elec-chrs}} = \pm 5 \text{ kcal mol}^{-1}$. The protein and the chain which contains the charged residues in a given plot are indicated in the upper left corner of the plot. The $\Delta\Delta G_{\text{elec-chrs}}$ value for each charged residue was calculated by using the continuum electrostatic methods described in the Experimental Section. The electrostatic profile of PfcCs shows less variabilities. In contrast, the DsCs electrostatic profile shows greater variations and a number of the residues have large stabilizing or destabilizing electrostatic free-energy contributions.

contributions between DsCs and PfcCs. 53 (30%) of the 176 charged residues in DsCs are significantly stabilizing or destabilizing. PfcCs contains 45 (out of 195, 23%) such residues. Based on the relative abundance of charged residues in PfcCs and DsCs, the expected number of charged residues with significantly stabilizing/destabilizing electrostatic free-energy contributions in PfcCs would be 59 if the two proteins had similar electrostatic profiles. Out of the 53 significantly stabilizing or destabilizing

charged residues in DsCs, 33 are significantly stabilizing and 20 are significantly destabilizing (33/20 = 1.65). In the case of PfcCs, 32 of the 45 charged residues with significant electrostatic free-energy contributions are stabilizing and the remaining 13 are destabilizing (32/13 = 2.46). These observations indicate that DsCs contains a greater proportion of significantly destabilizing charged residues (20 out of 176, 11.4%) than PfcCs (13 out of 195, 6.7%). 60% (12 out of 20) of these significantly destabilizing charged residues lie in the DsCs active site (Table 2, see below). The charged residues are exposed to similar extents in DsCs and PfcCs (data not shown). GgCs contains 55 (34%) charged residues with $|\Delta\Delta G_{\text{elec-chrs}}| \geq 5 \text{ kcal mol}^{-1}$ and the ratio of significantly stabilizing to significantly destabilizing residues is 2.23 (38/17).

Electrostatic free-energy contributions by salt bridges and their networks

Salt bridges were identified and several sets of calculations with different protein and water dielectric constants (ϵ_p and ϵ_w , respectively) have been carried out for the three citrate synthase structures. The Supporting Information gives the electrostatic strengths of salt bridges and their networks in PfcCs, DsCs, and GgCs.

26 salt bridges in DsCs have an average electrostatic free-energy contribution ($\Delta\Delta G_{\text{elec-SB}}$) of $-6.1 \pm 5.5 \text{ kcal mol}^{-1}$ at 25°C when calculated with ϵ_p and ϵ_w values of 4 and 80, respectively. If we change the ϵ_p value to 20 and the temperature to 0°C , the average $\Delta\Delta G_{\text{elec-SB}}$ value for the salt bridges in DsCs becomes $-2.2 \pm 1.2 \text{ kcal mol}^{-1}$ (with $\epsilon_p = 20$ and $\epsilon_w = 87.9$; Table S1a in the Supporting Information). Again, the above-average values are computed from several sets of electrostatic calculations on individual salt bridges and the large standard deviations about the average values indicate large scatter in the data due to the variabilities in the structural context, location in the protein, and orientation of the side-chain

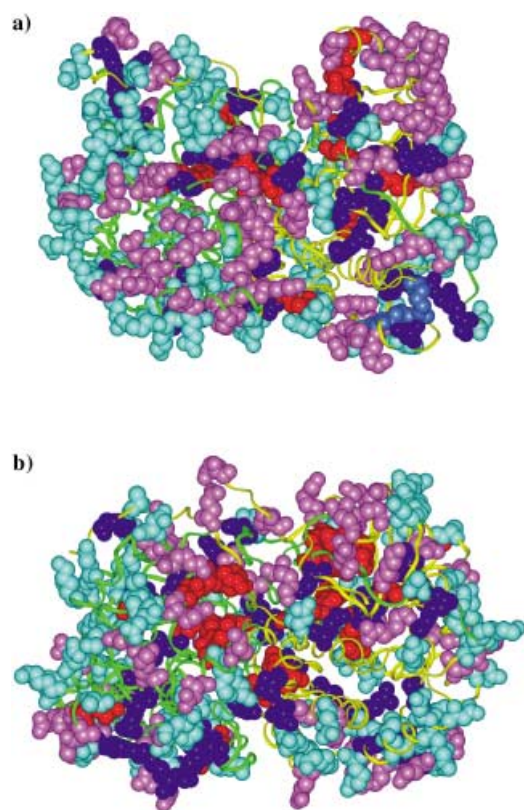


Figure 4. Diagrams showing the charged residues in the three-dimensional structures of a) hyperthermophilic (PfCs) and b) psychrophilic (DsCs) citrate synthases. In each case, the individual polypeptide chains are shown as green and yellow ribbons. The charged residues are shown as CPK representations in different colors according to their electrostatic free-energy contributions ($\Delta\Delta G_{\text{elec-chrs}}$). The charged residues with $\Delta\Delta G_{\text{elec-chrs}} < -5 \text{ kcal mol}^{-1}$ are shown in dark blue. The red-colored residues have $\Delta\Delta G_{\text{elec-chrs}} > 5 \text{ kcal mol}^{-1}$. The residues with $0 < \Delta\Delta G_{\text{elec-chrs}} < 5 \text{ kcal mol}^{-1}$ are shown in magenta. Cyan indicates the residues with $-5 < \Delta\Delta G_{\text{elec-chrs}} < 0 \text{ kcal mol}^{-1}$. Hence, the residues shown in magenta and red are destabilizing while those in blue and cyan are stabilizing. Note that DsCs contains more red- and blue-colored residues than PfCs; this indicates greater variabilities in the electrostatic profiles of DsCs. For the sake of clarity, other residues in both the citrate synthases are not shown.

functional groups in the charged residues in the individual salt bridges. All 26 salt bridges in DsCs are stabilizing. Each subunit contains two highly stabilizing salt bridges ($\Delta\Delta G_{\text{elec-SB}} < -10 \text{ kcal mol}^{-1}$). Both intersubunit salt bridges in DsCs are moderately stabilizing. The intrasubunit salt-bridge networks in both subunits of DsCs are marginally destabilizing when we use values of $\epsilon_p = 4$ and $\epsilon_w = 80$. However, when the ϵ_p value is changed to 20, the networks become marginally stabilizing (Table S1 d in the Supporting Information).

The 20 salt bridges in PfCs have an average electrostatic free-energy contribution ($\Delta\Delta G_{\text{elec-SB}}$) of $-4.0 \pm 4.1 \text{ kcal mol}^{-1}$ at 25°C with $\epsilon_p = 4$ and $\epsilon_w = 80$. If the ϵ_p value is changed to 20 and the temperature is raised to 100°C , the average $\Delta\Delta G_{\text{elec-SB}}$ value becomes $-3.2 \pm 1.5 \text{ kcal mol}^{-1}$. 18 out of the 20 salt bridges in PfCs are stabilizing. PfCs contains five intersubunit salt bridges. Two of these are highly stabilizing ($\Delta\Delta G_{\text{elec-SB}} < -10 \text{ kcal mol}^{-1}$; Table S1 b in the Supporting Information). Both intra- and intersubunit salt-bridge networks are stabilizing.

Arnott et al.^[17] have highlighted the complementarity of PfCs subunits (Figure 2). PfCs contains additional dimer interface interactions at the C terminus. The C terminus of each subunit of PfCs wraps around the other subunit and connects through intersubunit salt bridges between Arg375 and Glu48 on different chains. Our calculations show these salt bridges to be highly stabilizing. Additionally, the stabilizing intersubunit salt-bridge network formed by residues Asp113 in chain A with His93 and Lys217 in chain B of PfCs is also part of the five-residue intersubunit ion-pair network identified by crystallographers.^[14a] By using site-directed mutagenesis, Arnott et al.^[17] disrupted the intersubunit salt bridges and the intersubunit ion-pair networks in PfCs. This leads to a 3–5-fold increase in the rate of thermal inactivation, even though the enzyme activity remains unaffected.^[17]

12 salt bridges in mesophilic citrate synthase (GgCs) have an average electrostatic free-energy contribution of $-8.2 \pm 6.1 \text{ kcal mol}^{-1}$ at 25°C with $\epsilon_p = 4$ and $\epsilon_w = 80$. When the ϵ_p value is changed to 20, the contribution becomes $-3.1 \pm 1.5 \text{ kcal mol}^{-1}$. In GgCs, all salt bridges are stabilizing and the two intersubunit salt bridges are highly stabilizing (Table S1 c in the Supporting Information).

When we compare DsCs, PfCs, and GgCs, on average, the salt bridges are strongest in GgCs, weaker in DsCs, and weakest in PfCs at room temperature. This trend changes if we use $\epsilon_p = 20$ and account for the change in the water dielectric constant at the living temperatures of PfCs and DsCs (Table S1 a–c in the Supporting Information). The salt bridges then have comparable strengths in PfCs and GgCs but those in DsCs are, on average, weaker by 1 kcal mol^{-1} .

Charged residues in the active sites of PfCs and DsCs

The active site of citrate synthase binds citrate and coenzyme A (CoA). The binding site of citrate is conserved between PfCs and DsCs but there are important differences in the CoA binding site.^[10a] Both PfCs and DsCs dimers contain two active sites but each active site involves residues from both monomers for citrate binding (Figure 2). A visual comparison of the PfCs and DsCs structures indicates a more intimate interaction between the two subunits in PfCs than in DsCs (Figure 2a as compared to 2b). This observation is supported by the greater burial of protein surfaces in the dimer interface of PfCs (Table 1). The two active sites appear to lie nearer the dimer interface in PfCs than in DsCs. We have used LIGPLOTS, available in the PDBSum database (<http://www.biochem.ucl.ac.uk/bsm/pdbsum/index.html>), to identify the active-site residues in PfCs and DsCs. Only those residues that are in contact with citrate or CoA were considered.

Table 2 compares accessible surface areas and $\Delta\Delta G_{\text{elec-chrs}}$ values (at 25°C) of the charged residues in the active-site regions of DsCs and PfCs. With two exceptions, most of the active-site residues in DsCs have slightly greater accessible surface areas than the corresponding residues in the PfCs active site. The three conserved catalytic residues, His221, His269, and Asp320, in DsCs^[10a] are also slightly more accessible to water. Two of the three conserved catalytic residues, His221 and His269,

Table 2. Accessible surface area and $\Delta\Delta G_{\text{elec-chrs}}$ of charged active-site residues in DsCs and PFCs.^[a]

Residue	DsCs (1A59)		Residue	PFCs (1AJ8)	
	ASA [%]	$\Delta\Delta G_{\text{elec-chrs}}$ [kcal mol ⁻¹]		ASA [%]	$\Delta\Delta G_{\text{elec-chrs}}$ [kcal mol ⁻¹]
Chain A					
H221	15.2	+20.6	H223	13.1	+14.3
			K254	84.2	+3.4
K263	76.1	+6.1	K256	70.5	+5.8
H269	33.5	+19.2	H262	31.9	+10.5
			R263	21.3	+7.6
K273	67.4	+4.9	K266	45.2	+4.6
R278	6.9	+9.2	R271	2.8	+11.0
K313	58.9	+2.3	K305	74.6	+4.1
D320	8.5	-15.9	D312	7.3	-12.2
R345	2.1	+19.3	R337	2.2	+18.4
			R353	37.5	+2.3
R364	7.9	+15.0	R356	7.2	+10.3
Chain B					
H221	16.6	+19.8	H223	14.5	+14.3
			K254	86.3	+1.7
K263	77.3	+5.9	K256	73.5	+4.9
H269	31.4	+19.3	H262	27.5	+10.4
			R263	20.8	+6.6
K273	67.4	+4.8	K266	45.7	+4.4
R278	6.3	+10.6	R271	1.7	+8.8
K313	59.2	+1.9	K305	77.8	+3.8
D320	11.5	-16.0	D312	7.1	-4.6
R345	1.7	+19.9	R337	2.5	+15.5
			R353	43.1	+3.9
R364	6.6	+15.7	R356	8.1	+13.1

[a] Each residue is indicated by its single letter code and number in the amino acid sequence. The crystallographic asymmetric unit of DsCs contains a monomer. The atomic coordinates of the full DsCs dimer, generated from crystallographic symmetry operations, were taken from from EBI-MSD protein quaternary structure server (<http://msd.ebi.ac.uk/>). Single rows show structurally corresponding active-site charged residues in DsCs and PFCs. The $\Delta\Delta G_{\text{elec-chrs}}$ values were calculated with $\epsilon_p = 4$ and $\epsilon_w = 80$ and room temperature conditions. These values for the charged active-site residues were calculated without substrates.

are highly destabilizing in DsCs and PFCs and the third one, Asp320, is highly stabilizing. Consistently with the results of Elcock,^[18] all but one (Asp320 in DsCs and Asp312 in PFCs) of the active-site charged residues in DsCs and PFCs have destabilizing electrostatic free-energy contributions. Furthermore, most of the active-site charged residues are more destabilizing in DsCs than in PFCs (Table 2). Figure 5 compares the electrostatic free-energy contributions, $\Delta\Delta G_{\text{elec-chrs}}$, by the charged residues in the active sites of DsCs and PFCs. The comparison is restricted to only those charged residues which occupy structurally equivalent positions in the DsCs and PFCs structures. We have followed the residue numbering in DsCs in the comparison (Figure 5). The catalytically active histidines, His221 and His269, are significantly more destabilizing in DsCs. Asp320 is more stabilizing in DsCs than in PFCs. Active sites in DsCs and PFCs contain a conserved salt bridge (Asp276–Arg278 in DsCs, Asp269–Arg271 in PFCs) in each monomer. These conserved bridges have stabilizing electrostatic contributions in both DsCs and PFCs but they are more stabilizing in PFCs when compared at their respective

optimum living temperatures (Table S1a, b in the Supporting Information). The calculations were performed without ligands.

Discussion

From a mesophile-centric reference, it appears that thermophilic and psychophilic proteins face almost opposite challenges. At high temperatures, proteins may face conformational disorder. Chemical reaction rates increase and substrate stability may decrease. Thermophilic proteins need to counter these effects, especially near the active sites and at subunit interfaces. In contrast, at low temperatures there is reduced atomic mobility and lower protein and solvent entropy. Reaction rates are reduced and solvent viscosity is increased. Psychophilic enzymes need to be more efficient to maintain metabolic flux.^[6] In addition, the physical properties of water also change substantially at low and high temperatures (Table 3).

Citrate synthase is one of the few enzymes whose structures are available across the full range of living temperatures.^[10e] Interestingly, citrate synthase from the psychophile *Arthobacter* Ds2–3R shows a high degree of sequence and structural similarity to that from the hyperthermophile *Pyrococcus furiosus*. This suggests that the differences between PFCs and DsCs may be related to the differences in the living temperatures of their source organisms rather than to phylogeny. All three citrate synthases in our study show similar atomic packing and bury their nonpolar surface areas to similar extents. However, the proportions of charged residues and the number of salt bridges (and their networks) are higher in the psychophilic citrate synthase (DsCs) than the mesophilic homologue (GgCs). This observation was rather unexpected as studies based on homology modeling have predicted that psychophilic proteins would contain fewer salt bridges (for example, refs. [7, 19]). Moreover, Russell et al.^[10a] found that the electrostatic potential of DsCs differs from that of PFCs. Taken together, these facts suggest that the increased occurrence of charged residues and salt bridges in the psychophilic citrate synthase (DsCs) may also be related to its adaptation to the cold temperatures.

Methods based on continuum electrostatics are often used to estimate the electrostatic free-energy contributions made by individual charged residues, by salt bridges, and by salt-bridge networks toward protein stability (for example, refs. [3f, 20]). In recent years, such calculations have found many application-^[3a, 20a,b, 21] and have proved to be useful in understanding protein thermostability.^[2c, 3d–f] The advantages and limitations of such calculations have been discussed earlier.^[20a, d, 22, 23] The results of the calculations depend upon the oligomeric state of the protein, temperature, pH value, and ionic strength. We have used the dimeric forms of all citrate synthases in the electrostatic calculations. All of our calculations assume conditions of room temperature, pH 7, and zero ionic strength. This facilitates direct comparison of the results for the psychophilic, mesophilic, and hyperthermophilic citrate synthases. In the case of salt bridges and their networks, the effect of temperature is taken into account by recalculating with the appropriate water dielectric constants and conversion factors. We have not scaled the atomic

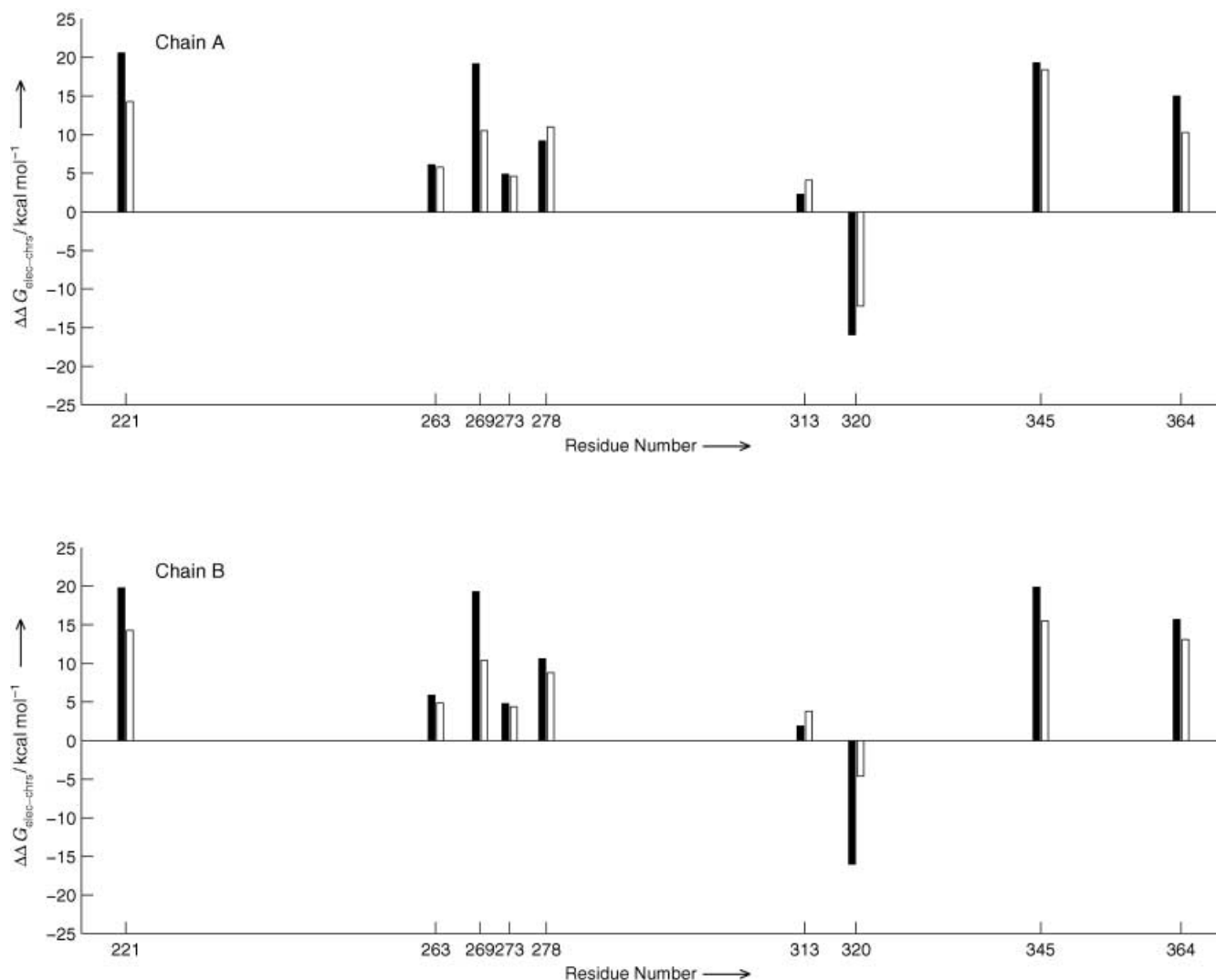


Figure 5. Bar diagrams comparing the electrostatic free-energy contributions ($\Delta\Delta G_{\text{elec-chrs}}$) by the charged residues in the active sites of the hyperthermophilic (PFCs; white bars) and psychrophilic (DsCs; black bars) citrate synthases. The comparison is restricted to only those charged residues that occupy structurally equivalent positions in PFCs and DsCs (Table 2). One bar diagram is plotted per polypeptide chain in the citrate synthase dimers. The residue numbers shown are for charged residues in DsCs active site. The residue numbers for the structurally corresponding PFCs charged residues can be obtained from Table 2. The charged residues with $\Delta\Delta G_{\text{elec-chrs}} > 0$ are destabilizing while those with $\Delta\Delta G_{\text{elec-chrs}} < 0$ are stabilizing. Most active-site charged residues are destabilizing in both PFCs and DsCs. However, those in DsCs are more destabilizing, especially the catalytically active histidines, His221 and His269. The $\Delta\Delta G_{\text{elec-chrs}}$ values for the charged residues in PFCs and DsCs were computed for room temperature conditions to facilitate a direct comparison. At the respective growth temperatures of PFCs and DsCs, the $\Delta\Delta G_{\text{elec-chrs}}$ values of the charged residues will change slightly since the dielectric constant of water decreases to 55.51 at 100 °C and increases to 87.9 at 0 °C. Due to this the PFCs active-site charged residues should become less destabilizing while those in DsCs should become more destabilizing, further enhancing the differences between the electrostatic properties of the active sites in the two proteins.

Table 3. Temperature-dependent variations in the physical properties of water.^[a]

Property	Temperature [°C]			
	0	20	40	100
dielectric constant	87.90	80.20	73.17	55.51
viscosity [$\mu\text{Pa}\cdot\text{s}$]	1793	1002	653.2	281.8
density [$\text{g}\cdot\text{cm}^{-3}$]	0.9998	0.9982	0.9922	0.9584
ΔC_p [$\text{J}\cdot\text{g}^{-1}\cdot\text{K}$]	4.22	4.18	4.17	4.22
surface tension [$\text{mN}\cdot\text{m}^{-1}$]	75.64	72.75	69.60	58.91

[a] Data taken from ref. [16]. The viscosity of water at 0 °C is nearly sixfold greater than that at 100 °C. Pa·s stands for Poiseuille, a unit for the coefficient of viscosity. The units of surface tension, $\text{mN}\cdot\text{m}^{-1}$, are millinewtons per meter. This is equivalent to dynes per centimeter.

radii to different temperatures as suggested by Elcock and McCammon.^[3d] The scaling factors are available for the temperature range of 5–100 °C, but the living temperature of the psychrophile is 0 °C. Nevertheless, the resulting differences are expected to be small. That our calculations are on the right track is also suggested by their consistency with the experimental results of Arnott et al.^[17]

At the coarse level, PFCs and DsCs appear to possess similar electrostatic properties. Both contain greater proportions of charged residues, salt bridges, and networks than mesophilic GgCs. The salt bridges and their networks are stabilizing in both PFCs and DsCs. In both, most of the active-site charged residues are destabilizing. However, there are important electrostatic

differences between PFCs and DsCs. DsCs contains a greater proportion of charged residues with large destabilizing electrostatic free-energy contributions. The active-site charged residues in DsCs show greater extents of destabilization. The location of the salt bridges and their networks are different. In PFCs, they tend to be more frequently at the dimer interface and near the active sites. In DsCs they are more distributed throughout the structure (Figure 2).

Table 3 compares the temperature dependence of the physical properties of water. At high temperatures, PFCs needs to guard against the loss of the native structure, particularly around the active site and at the subunit interface, due to increased atomic mobility. PFCs may use increased stabilizing electrostatic interactions, particularly in these regions to resist disorder. Due to the lower surface tension and viscosity of water, it is easier for the substrate molecules to diffuse toward the enzyme active site at high temperatures. Yet, it may also be more difficult to retain them. The active sites of PFCs are larger and lie further into the dimer interface. The presence of a longer loop at the entrance of each PFCs active site^[10a] may also be useful in trapping the substrate molecules at high temperatures.

In the absence of chemical denaturants, proteins normally do not cold denature around 0 °C, the typical living temperature of the psychrophiles. The calculated cold denaturation temperatures in a dataset of 26 unique two-state proteins had an average value of 233 K (−40 °C).^[24a] What then is the possible role of electrostatics in adaptation to cold? At temperatures of approximately 0 °C, water has significantly higher viscosity and surface tension. Water is almost twice as viscous at 0 °C as at room temperature. This fact indicates the presence of optimum hydrogen-bonding networks in the water structure at low temperatures. Furthermore, the solubilities of several naturally occurring amino acids with hydrophobic side chains remain low and are almost constant between 0–30 °C, a fact making most proteins maximally stable around room temperature.^[24] Combining these observations, it appears that the dissolution of a protein molecule in water at low temperatures will incur a larger energetic cost as it would require the disruption of optimal hydrogen-bonding networks in the water structure. This energetic cost may be offset if the protein's surface is decorated with charged residues as in DsCs. These charged residues may form favorable electrostatic interactions with the surrounding water molecules along with those among the charged residues themselves.

The diffusion of substrate molecules to the enzyme active site and the chemical reaction rates may be slower around 0 °C.^[6c] Consistently, the active-site residues in DsCs have slightly larger accessible surface areas (Table 2). The higher catalytic efficiency of psychrophilic enzymes may originate from their greater flexibility.^[6] The crystallographic *B* factors can potentially estimate the atomic mobility in proteins. In the case of DsCs, the *B* factors do not yield clues about the greater flexibility of DsCs relative to GgCs and PFCs (Table 1; ref. [10a]). Nevertheless, the *B* factors for main-chain and side-chain atoms in the catalytic domain of each DsCs monomer are larger, a fact indicating that this domain may be more flexible than the rest of the DsCs structure.^[10e]

Our continuum electrostatic calculations on the charged residues in the PFCs and DsCs active sites indicate that most of the charged residues in this region are electrostatically destabilizing to both proteins. The extent of destabilization is lower in PFCs and would further decrease at 100 °C due to the decrease in the water dielectric constant. On the other hand, the extent of destabilization by the charged active-site residues in DsCs is larger, possibly contributing to the greater active-site flexibility. The instability of the active-site residues is often related to their mobility, as shown for the mobile HIV-1 protease flaps.^[25]

In summary, protein electrostatics may play important roles in both heat and cold adaptation of citrate synthase. The hyperthermophilic citrate synthase may use electrostatics to guard against thermal denaturation and to preserve its dimeric state and active site at high temperatures. On the other hand, the psychrophilic citrate synthase possibly uses electrostatics to ensure proper solvation at low temperatures and to impart greater flexibility, particularly in the active-site region.

Manipulation of protein electrostatics has been exploited by the thermophilic proteins to adapt to high temperatures.^[1a, 2b, c, 3a] Here, we have proposed that psychrophilic proteins may also use electrostatics as an adaptation strategy. While it is difficult to substantiate the role of electrostatics in cold adaptation, owing to the availability of only a handful of protein structures from psychrophiles, nevertheless, supportive evidence is derived from additional consistent examples. Malate dehydrogenase appears to be a second example where electrostatics may play important roles both in heat and cold adaptation.^[10b] In this case again, the psychrophilic *Aquaspirillum arcticum* malate dehydrogenase shows high sequence and structural similarity with the thermophilic *Thermus flavus* malate dehydrogenase. *A. arcticum* malate dehydrogenase also has higher active-site flexibility and greater distribution of charges on the protein surface than the thermophilic malate dehydrogenase. The two malate dehydrogenases also contain a similar number of hydrogen bonds, salt bridges/ion pairs, and salt-bridge networks, but the distributions of these electrostatic interactions are different.^[10b] Brandsdal et al.^[26] have reported that electrostatics play an important role in the cold adaptation of salmon trypsin. The availability of additional data will help further investigations in this regard.

Experimental Section

Multiple sequence comparison of citrate synthase: SEQWEB, a web interface for programs in the GCG package, was used. SEQWEB is available as a web-runnable program from the <http://www.fbsc.ncifcrf.gov> web site. The sequences of citrate synthase (E.C. 4.1.3.7) were retrieved from the SWISS-PROT database by using the LOOKUP program. Entries containing only sequence fragments were ignored. Sequences in 44 selected entries were multiply aligned by using the Blosum 62 matrix^[27] with a Gap creation penalty of 8 and Gap extension penalty of 2. The GROWTREE program in the EVOLUTION module was used to generate the phylogram presented in the Supporting Information. To individually compare the amino acid sequences of the psychrophilic citrate synthase with those from other organisms, the GAP program was used.

Citrate synthase structures and their comparison: Three high-resolution crystal structures of citrate synthase were selected from the PDB.^[13] These were from psychrophilic *Arthobacter* Ds2–3R (DsCs; PDB file no.: 1A59, 2.09 Å resolution), chicken (GgCs; PDB file no.: 1CSH, 1.6 Å resolution), and hyperthermophilic *Pyrococcus furiosus* (PFCs; PDB file no.: 1AJ8, 1.9 Å resolution). The biologically active unit is a dimer in all three cases. However, the crystallographic asymmetric units for the psychrophilic and mesophilic structures contain only monomers. The complete dimeric forms for these molecules were obtained from the EBI-MSD protein quaternary structure server (<http://msd.ebi.ac.uk/>). Quaternary structures on this server are generated by applying the crystallographic symmetry operations on the asymmetric unit. In all of the three crystal structures, citrate synthase is in a closed conformation. The three structures were aligned by using the HOMOLOGY module in the INSIGHTII (version 2000) package. The Access Surf program in the ProStat group in the HOMOLOGY module of the INSIGHTII package was used to compute the polar and nonpolar accessible surface areas.

Calculation of structural parameters: The hydrophobicity, compactness, number of hydrogen bonds, and salt bridges in each of the three citrate synthases were calculated. The hydrophobicity is computed as the ratio of buried nonpolar surface area to the total nonpolar surface area.^[28] It measures the extent to which a protein buries its nonpolar surface area. Compactness is defined as the ratio of the volume of the protein to the volume of the sphere that has the same surface area as the protein.^[28] Compactness indicates the goodness of atomic packing in the protein structures. Hydrogen-bond formation was inferred if the distance between a pair of nonbonded nitrogen and oxygen atoms (Donor (D)–Acceptor (A) pairs) was within 3.5 Å. The geometrical goodness of the hydrogen bond was assessed by computing two angles: angle θ_D between vectors BD–D and D–A, where BD is the atom covalently bonded to the donor atom, and angle θ_A between vectors D–A and A–BA, where BA is the atom covalently bonded to the acceptor atom. A hydrogen bond was taken to have a good geometry if both angles lie in the range 90°–150°. Only those hydrogen bonds which have a good geometry were included.^[2b] Salt-bridge formation between a pair of oppositely charged (Asp and Glu versus Arg, Lys, and His) residues was inferred following two criteria: 1) at least one pair of charged-residue side-chain nitrogen and oxygen atoms is within 4.0 Å and 2) the side-chain charged-group centroids are within 4.0 Å. The centroid positions of the side-chain charged groups in the charged residues were computed by using the heavy (non-hydrogen) atomic coordinates in the charged groups.^[20b]

Continuum electrostatic calculations: We have computed the electrostatic contribution of charged residues, salt bridges, and salt-bridge networks toward protein stability with respect to the corresponding hydrophobic isosteres. The hydrophobic isosteres are the charged residues with all partial atomic charges in the side chain set to zero.^[20a, d] The total electrostatic contribution of a charged residue toward protein stability ($\Delta\Delta G_{\text{elec-chrs}}$) is given by the sum of $\Delta\Delta G_{\text{dolv-chrs}}$ and $\Delta\Delta G_{\text{prt-chrs}}$,^[20d] where $\Delta\Delta G_{\text{dolv-chrs}}$ is the free-energy penalty paid due to desolvation of the charged residue in the folded state of the protein as compared to the unfolded state and $\Delta\Delta G_{\text{prt-chrs}}$ is the free-energy change due to interaction of the charged residue with all the partial atomic charges in the rest of the protein in the folded state.

The protein structures were prepared for the continuum electrostatic calculations by adding hydrogen atoms, capping the polypeptide chains, and defining the protonation states of all the charged residues at pH 7. Histidines were taken in their unprotonated form. The BIOPOLYMER module in the INSIGHTII (version 2000) package

was used for this purpose. The hydrogen-atom positions in the each structure were optimized by performing energy minimizations of the structure while keeping the positions of heavy (non-hydrogen) atoms fixed. The minimization routines consisted of 100 cycles of steepest descent followed by 500 cycles of conjugate gradient. These were performed in vacuo with distance-dependent dielectric values by using the DISCOVER module in the INSIGHTII package. This procedure improves the accuracy of the continuum electrostatic calculations.^[29] The electrostatic calculations were performed by using the DELPHI package^[30] and the PARSE3 set of partial atomic charges and atomic radii.^[31] Each protein was mapped onto a grid with spacing of 0.83333 Å. Initially a rough grid was calculated by using full coulombic boundary conditions, to obtain a focused grid with a solute (protein) extent of 95%. All the electrostatic calculations assumed conditions of room temperature (25 °C), pH 7, and zero ionic strength. The calculations for the electrostatic free-energy contributions by the individual charged residues in PFCs, DsCs, and GgCs were performed with the protein dielectric constant (ϵ_p) and water dielectric constant (ϵ_w) set at 4 and 80, respectively.

The calculations for electrostatic free-energy contributions by salt bridges and their networks were performed in an analogous way with additional energy terms describing the interaction among the charged residues forming the salt bridges and networks. The methods for these calculations are explained in the Supporting Information. The results of all our electrostatic calculations are presented in units of kcal mol⁻¹. The corresponding conversion for SI units is 1 cal = 4.18 J.

Acknowledgements

We thank Dr. Neeti Sinha, Dr. Chung Jung Tsai, Dr. Kannan Gunasekaran, Dr. David Zanuy, and, in particular, Dr. Jacob V. Maizel for numerous helpful discussions. Dr. Buyong Ma is thanked for help in figure preparation. The research of R.N. in Israel has been supported in part by the “Center of Excellence in Geometric Computing and its Applications” funded by the Israel Science Foundation, by a Ministry of Science grant, by the Adams Brain Center, and by Tel Aviv University Basic Research grants. This project has been funded in whole or in part with Federal funds from the National Cancer Institute, the National Institutes of Health, under contract number NO1-CO-12400. The content of this publication does not necessarily reflect the view or policies of the Department of Health and Human Services, nor does mention of trade names, commercial products, or organization imply endorsement by the US Government.

Keywords: citrate synthases • electrostatic interactions • protein structures • psychrophiles • thermophiles

- [1] a) S. Kumar, R. Nussinov, *Cell. Mol. Life Sci.* **2001**, *58*, 1216–1233; b) R. Sterner, W. Liebl, *Crit. Rev. Biochem. Mol. Biol.* **2001**, *36*, 39–106; c) D. Perl, F. X. Schmid, *ChemBioChem* **2002**, *3*, 39–44.
- [2] a) S. Kumar, C. J. Tsai, R. Nussinov, *Biochemistry* **2001**, *40*, 14152–14165; b) S. Kumar, C. J. Tsai, R. Nussinov, *Protein Eng.* **2000**, *13*, 179–191; c) S. Kumar, B. Ma, C. J. Tsai, R. Nussinov, *Proteins: Struct. Funct. Genet.* **2000**, *38*, 368–338; d) A. Szilagyi, P. Zavodszky, *Structure Fold. Des.* **2000**, *8*, 493–504; e) S. Chakravarty, R. Varadarajan, *Biochemistry* **2002**, *41*, 8152–8161.
- [3] a) S. Kumar, R. Nussinov, *ChemBioChem* **2002**, *3*, 604–617; b) J. M. Sanchez-Ruiz, G. I. Makhatadze, *Trends Biotechnol.* **2001**, *19*, 132–135;

- c) D. Perl, F. X. Schmid, *J. Mol. Biol.* **2001**, *313*, 343–357; d) A. H. Elcock, J. A. McCammon, *J. Phys. Chem. B* **1997**, *101*, 9624–9634; e) A. H. Elcock, *J. Mol. Biol.* **1998**, *284*, 489–502; f) L. Xiao, B. Honig, *J. Mol. Biol.* **1999**, *289*, 1435–1444.
- [4] D. Perl, U. Mueller, U. Heinemann, F. X. Schmid, *Nature Struct. Biol.* **2000**, *7*, 380–383.
- [5] a) N. J. Russell, *Extremophiles* **2000**, *4*, 83–90; b) G. Gianese, P. Argos, S. Pascarella, *Protein Eng.* **2001**, *14*, 141–148.
- [6] a) L. Zecchinon, P. Claverie, T. Collins, S. D'Amico, D. Delille, G. Feller, D. Georlette, E. Gratia, A. Hoyoux, M. A. Meuwis, G. Sonan, C. Gerday, *Extremophiles* **2001**, *5*, 313–321; b) C. Gerday, M. Aittaleb, J. L. Arpigny, E. Baise, J. P. Chessa, G. Garsoux, I. Petrescu, G. Feller, *Biochim. Biophys. Acta* **1997**, *1342*, 119–131; c) G. Feller, C. Gerday, *Cell. Mol. Life Sci.* **1997**, *53*, 830–841.
- [7] G. Wallon, S. T. Lovett, C. Magyar, A. Svingor, A. Szilagyi, P. Zavodszky, D. Ringe, G. A. Petsko, *Protein Eng.* **1997**, *10*, 665–672.
- [8] C. H. Chen, D. S. Berns, *Biophys. Chem.* **1978**, *8*, 203–213.
- [9] T. Lonhienne, J. Zoidakis, C. E. Vorgias, G. Feller, C. Gerday, V. Bouriotis, *J. Mol. Biol.* **2001**, *310*, 291–297.
- [10] a) R. J. M. Russell, U. Gerike, M. J. Danson, D. W. Hough, G. L. Taylor, *Structure* **1998**, *6*, 351–361; b) S. Y. Kim, K. Y. Hwang, S. H. Kim, H. C. Sung, Y. S. Han, Y. Cho, *J. Biol. Chem.* **1999**, *274*, 11 761–11 767; c) D. Maes, J. P. Zeelen, N. Thanki, N. Beaucamp, M. Alvarez, M. H. Thi, J. Backmann, J. A. Martial, L. Wyns, R. Jaenicke, R. K. Wierenga, *Proteins: Struct. Funct. Genet.* **1999**, *37*, 441–453; d) L. H. K. Schroder, N. P. Willassen, A. O. Smalas, *Eur. J. Biochem.* **2000**, *267*, 1039–1049; e) U. Gerike, M. J. Danson, D. W. Hough, *Protein Eng.* **2001**, *14*, 655–661.
- [11] *Biochemical pathways: An atlas of biochemistry and molecular biology* (Ed.: G. Michal), Wiley, New York, **1999**, pp. 43.
- [12] K. C. Usher, S. J. Remington, D. P. Martin, D. G. Drueckhammer, *Biochemistry* **1994**, *33*, 7753–7759.
- [13] F. C. Bernstein, T. F. Koetzle, G. J. Williams, E. E. Myer, Jr., M. D. Brice, J. R. Rodgers, O. Kennard, T. Shimanoouchi, M. Tasumi, *J. Mol. Biol.* **1977**, *112*, 535–542.
- [14] a) R. J. M. Russell, J. M. C. Ferguson, D. W. Hough, M. J. Danson, G. L. Taylor, *Biochemistry* **1997**, *36*, 9983–9994; b) M. J. Danson, D. W. Hough, *Methods Enzymol.* **2001**, *331*, 3–12.
- [15] S. Kumar, M. Bansal, *Proteins: Struct. Funct. Genet.* **1998**, *31*, 460–476.
- [16] *CRC Handbook of Chemistry and Physics*, 82nd ed. (Ed.: D. R. Lide), CRC Press, Washington DC, **2001**, p. 6.
- [17] M. A. Arnott, R. A. Michael, C. R. Thompson, D. W. Hough, M. J. Danson, *J. Mol. Biol.* **2000**, *304*, 657–668.
- [18] A. H. Elcock, *J. Mol. Biol.* **2001**, *312*, 885–896.
- [19] T. Thomas, R. Caviccholi, *FEBS Lett.* **1998**, *439*, 281–286.
- [20] a) Z. S. Hendsch, B. Tidor, *Protein Sci.* **1994**, *3*, 211–226; b) S. Kumar, R. Nussinov, *J. Mol. Biol.* **1999**, *293*, 1241–1255; c) S. Kumar, R. Nussinov, *Proteins: Struct. Funct. Genet.* **2000**, *41*, 485–497; d) S. Spector, M. Wang, S. A. Carp, J. Robblee, Z. S. Hendsch, R. Fairman, B. Tidor, D. P. Raleigh, *Biochemistry* **2000**, *39*, 872–879.
- [21] a) B. Honig, A. Nicholls, *Science* **1995**, *268*, 1144–1149; b) S. Kumar, R. Nussinov, *Proteins: Struct. Funct. Genet.* **2001**, *43*, 433–454; c) V. Lounnas, R. C. Wade, *Biochemistry* **1997**, *36*, 5402–5417; d) D. Xu, S. L. Lin, R. Nussinov, *J. Mol. Biol.* **1997**, *265*, 68–84.
- [22] C. N. Schutz, A. Warshel, *Proteins: Struct. Funct. Genet.* **2001**, *44*, 400–417.
- [23] a) C. D. Waldburger, J. F. Schildbach, R. T. Sauer, *Nature Struct. Biol.* **1995**, *2*, 122–128; b) C. D. Waldburger, T. Jonsson, R. T. Sauer, *Biochemistry* **1996**, *35*, 2629–2634.
- [24] a) S. Kumar, C. J. Tsai, R. Nussinov, *Biochemistry* **2002**, *41*, 5359–5374; b) *Handbook of Biochemistry and Molecular Biology*, 3rd ed., (Ed.: G. D. Fasman), CRC Press, Cleveland, **1976**, pp. 114–115.
- [25] M. J. Todd, E. Freire, *Proteins: Struct. Funct. Genet.* **1999**, *36*, 147–156.
- [26] B. O. Brandsdal, A. O. Smalas, J. Aqvist, *FEBS Lett.* **2001**, *499*, 171–175.
- [27] S. Henikoff, J. G. Henikoff, *Proc. Natl. Acad. Sci. USA* **1992**, *89*, 10915–10919.
- [28] a) C. J. Tsai, R. Nussinov, *Protein Sci.* **1997**, *6*, 1426–1437; b) C. J. Tsai, R. Nussinov, *Protein Sci.* **1997**, *6*, 24–42.
- [29] J. E. Nielsen, K. V. Anderson, B. Honig, R. W. W. Hooft, G. Klebe, G. Vriend, R. C. Wade, *Protein Eng.* **1999**, *12*, 657–662.
- [30] a) M. K. Gilson, A. Rashin, R. Fine, B. Honig, *J. Mol. Biol.* **1985**, *183*, 503–516; b) M. K. Gilson, K. A. Sharp, B. H. Honig, *J. Comp. Chem.* **1988**, *9*, 327–335.
- [31] D. Sitkoff, K. A. Sharp, B. Honig, *J. Phys. Chem.* **1994**, *98*, 1978–1988.

Received: April 17, 2003

Revised: October 16, 2003 [F627]